Astron. Astrophys. 170, 120–125 (1986)

ASTRONOMY
AND
ASTROPHYSICS

Some effects of finite spectral resolution on the Stokes *V* profile

S.K. Solanki and J.O. Stenflo

Institute of Astronomy, ETH-Zentrum, CH-8092 Zürich, Switzerland

Received March 13, accepted June 13, 1986

Summary. The effects of finite spectral resolution on different parameters of the Stokes *V* profile are studied by convoluting spectrally resolved Stokes *V* profiles (observed with an FTS) with model instrumental profiles of varying width and shape. It is found that not only the area and amplitude of Stokes *V* decrease strongly with increased spectral smearing, but that the asymmetries of amplitude and area are also affected. Ways of defining these quantities in a resolution independent manner are considered. A strong dependence of the zero-crossing wavelength on the spectrograph entrance slit width is noticed. The resolution induced wavelength shift is always towards the red, giving rise to fictitious downflows in observations with low spectral resolution. By modelling this effect using the estimated instrumental parameters employed by different authors it is shown that the observations of the Stokes *V* zero-crossing wavelength in the literature are consistent with an absence of downflows larger than about 250 m s^{-1} inside the fluxtubes.

Key words: Stokes parameters – spectral resolution – fluxtubes – downflows

1. Introduction

In their quest for better data, solar observers have often opted for increased spatial and temporal resolution at the cost of a certain amount of spectral resolution. As long as the observations are limited to measurements of spectral intensity (Stokes *I*), this usually does not present a serious problem (except for the detailed analysis of the line profile, its bisector, and related studies). The profile is broadened, the line depth is reduced, but the equivalent width and the core wavelength remain relatively unaffected. The situation changes dramatically for the cases when circularly polarized spectra (Stokes *V*) are required, e.g. for problems relating to the diagnostics of the properties of solar magnetic fluxtubes. Not only are the amplitude and asymmetry of a Stokes *V* line profile affected by changes in spectral resolution, but also the areas of both its wings, and the wavelength of its zero-crossing. Another reason why the magnitude of the observed effect on Stokes *V* is generally larger than on Stokes *I* is due to the circumstance that with most instruments, the measurement of Stokes *V* requires wide slits to get a good signal to noise ratio while maintaining high temporal and/or spatial resolution. Even in the optimum spectral lines the Stokes *V* amplitude seldom exceeds a few percent of the continuum intensity when observing outside sunspots.

In the present paper we shall consider some general effects of spectral smearing on the Stokes *V* profile of the Fe I 5250.2 Å line, as observed on the sun with a Fourier transform spectrometer (FTS) at a very high spectral resolution. The effects of low spectral resolution will be numerically simulated by convoluting these observed line profiles with model instrumental profiles. We shall also try to find some Stokes *V* parameters which are insensitive to the spectral resolution. Finally, we shall show that the large Stokes *V* zero-crossing wavelength shifts observed by Wiehr (1985a) and by Scholier and Wiehr (1985) from complete profiles, and by Giovanelli and Slaughter (1978) with the line-centre-magnetogram technique of Giovanelli and Ramsey (1971) are compatible with the results of Stenflo and Harvey (1985) and Solanki (1985, 1986), who find much smaller shifts. These apparently different results can be understood in terms of differences in the spectral resolution used by the various observers, and partly also as a result of the granular blueshift of the Stokes *I* profiles.

2. Description of the technique and input data

We have used data with very high spectral resolution as our starting point, and have simulated the effect of a finite entrance slit width and finite grating resolution by convoluting the data with an instrumental spectral profile. Using instrumental profiles of slightly different shapes we have also been able to get an impression of how large the effect of the profile shape is on the results. We have used a Gaussian, as well as Voigt profiles with 'damping constants' $a = 0.1$ and $a = 0.2$ (see Mihalas, 1978, for a definition of the Voigt profile), for the total instrumental profile. Allen (1973) and Unsöld (1955) give the following relation between v, the width of the Gaussian at the point where its value has fallen to $1/e$ (i.e. the Doppler width), and the entrance slit full width, s: $v = 0.41s$. For a perfect spectrograph with infinitely narrow entrance and exit slits the relations given by Allen are $v = 0.43l$, and $a = 0.33$, where l is the resolving distance (i.e. the distance from the central maximum to the first minimum), and v and a are the 'Doppler width' and 'damping constant' of a Voigt profile.

Send offprint requests to: S.K. Solanki

The reason why we have chosen these approximate profile shapes instead of theoretically more exact ones involving convolutions between sinc^2 and rectangular functions, is that different ratios of entrance to exit slit width and spectrograph resolving power result in different instrumental profile shapes which can only be described by introducing a larger number of free parameters. We feel that such a detailed analysis lies beyond the scope of the present paper, for the following reasons. Firstly, the theoretical apparatus function can differ considerably from the profile of a real instrument, which can be asymmetric, with grating and lense defects also contributing significantly to it (Unsöld, 1955, von Alvensleben, 1957). Secondly, as shall be apparent from the results in Sect. 3, the shape of the apparatus function generally plays a minor role, compared to other parameters like its width, or the asymmetry of Stokes V, etc..

The technique describe above was used on data obtained on April 29 and 30 with the Kitt Peak McMath telescope and the 1-m FTS adapted to record Stokes I and V simultaneously. The spectra containing the Fe I 5250.2 Å profile were obtained in a strong active region plage at $\mu = 0.92$, and in an enhanced network element at $\mu \approx 1.00$. Their spectral resolution of 420 000 is large enough to ensure that the solar line profiles are completely resolved. The Stokes V signal to noise ratio of the Fe I 5250.2 Å Stokes V peak is approximately 100 for the enhanced network and 300 for the plage. The observations have been described in greater detail by Stenflo et al. (1984), and we refer to that paper for additional information.

The Fe I 5250.2 Å line was chosen mainly for the reason that it was, and still is, one of the most widely used lines for polarimetric observations of all kinds, e.g. for magnetograph observations and magnetic field strength determinations using the line ratio technique. It is also free of obvious blends out to about 0.2 Å in both wings. In Fig. 1 the Stokes V profile of Fe I 5250.2 Å is shown convoluted with different Gaussian instrumental profiles having widths, v, ranging from 0 mÅ (corresponding to the original FTS spectrum; the highest and narrowest profile in the figure) to 150 mÅ (the flattest and broadest profile). The width of the instrumental Gaussian has been increased in steps of 10 mÅ.

3. Results

3.1. Amplitude, area, and asymmetry

One of the qualitative results is readily visible from Fig. 1; the amplitude of the Stokes V profile decreases rapidly with increasing spectral smearing. The quantitative form of this decline is shown in Fig. 2, where the Stokes V amplitude, normalised to its value for the fully resolved profile, i.e. $(a_b(v) + a_r(v))/(a_b(v = 0) + a_r(v = 0))$, as well as the total normalised area of the V profile $(A_b(v) + A_r(v))/(A_b(v = 0) + A_r(v = 0))$, have been plotted vs. v, the width of the instrumental profile. A_b, A_r, a_b and a_r are the blue and red *absolute* areas and amplitudes of Stokes V. The three different model instrumental profile shapes chosen are: a Gaussian (solid line), a Voigt profile with 'damping constant' $a = 0.1$ (dashed line), and a Voigt profile with $a = 0.2$ (dash-dotted line). These profiles will be represented in the same manner in the remaining figures, unless it is explicitly stated otherwise. Figure 2 shows that the amplitude and area decrease more rapidly when the wings of the instrumental profile are more pronounced. Although this effect is not negligible, it is nevertheless small compared to the effect of increasing v, and supports the assumption that the exact profile shape is not very important. The curves obtained from the network and active region profiles are practically identical, and have therefore not been plotted separately. It should be noticed that for lines narrower than Fe I 5250 the effect will be even larger. Therefore only filling factors determined by procedures which account for finite spectral resolution, e.g.

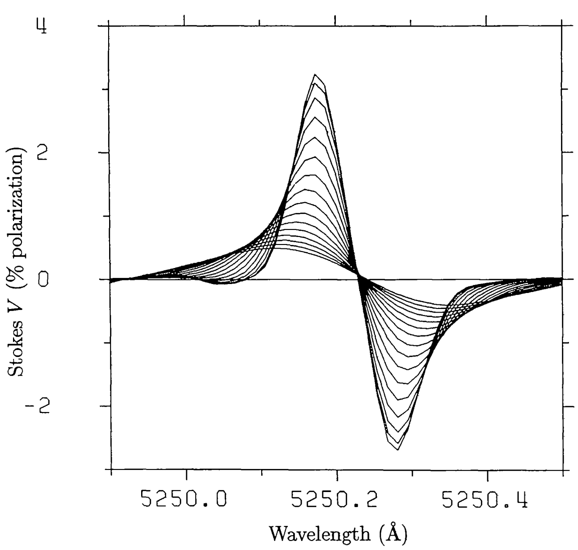

Fig. 1. Stokes V profile of Fe I 5250.2 Å for different amounts of spectral smearing. The highest and narrowest profile represents the original FTS data. The other profiles have been convoluted with increasingly broader Gaussians representing instrumental smearing. The broadest Gaussian has $v = 150$ mÅ, where v is the e-folding width ('Doppler' width)

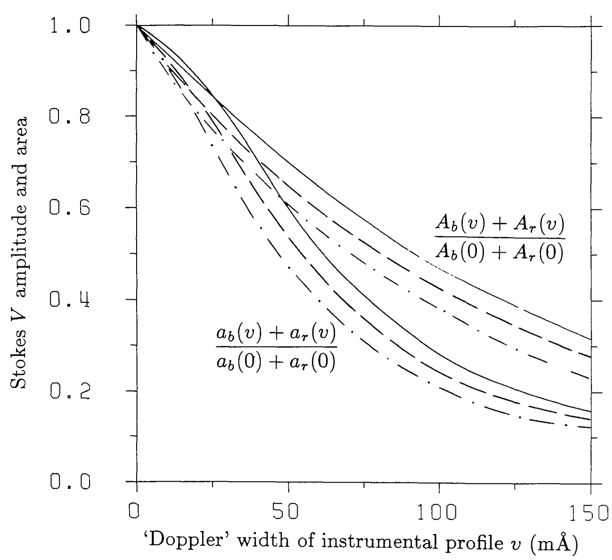

Fig. 2. Sum of the absolute blue and red amplitudes and of the blue and red areas of Stokes V vs. 'Doppler' width v (in mÅ) of the instrumental profile. The Stokes V amplitude (resp. area) has been normalised to its value at $v = 0$. Solid line: Gaussian apparatus function. Dashed line: Voigt apparatus function (with damping constant, $a = 0.1$). Dot-dashed line: Voigt apparatus function ($a = 0.2$). The curves represent the Fe I 5250.2 Å line in plage as well as network regions

from the ratio of V amplitude to $dI/d\lambda$ at the same wavelength, should not be appreciably affected by spectral smearing.

The decrease in Stokes V area is not quite as strong as the decrease in Stokes V amplitude, but is still considerable. This decrease of the area has a simple intuitive explanation. Due to the instrumental broadening the two wings of Stokes V overlap and cancel each other increasingly, thus producing the observed result. Physically this is related to the fact that the absolute areas of the two Stokes V wings play a role very similar to that of the line depth of the I profile, and *not* to that of its equivalent width.

In our search for a resolution independent parameter, we find that S_V, the area of the lower half of the I_V profile (cf. Solanki and Stenflo, 1984, 1985 for a definition of the I_V profile), decreases by less than 10% between $v = 0$ and $v = 150$ mÅ. For the range $0 \leq v \leq 50$ mÅ the decrease is less than 1%. S_V is therefore a quantity, which can be used to determine the filling factor almost independently of the spectral resolution used.

The Stokes V asymmetry is also affected by spectral smearing. Figure 3 shows the change in Stokes V relative area asymmetry, $(A_b - A_r)/(A_b + A_r)$, and the relative amplitude asymmetry, $(a_b - a_r)/(a_b + a_r)$, induced by changing v (for an active region plage). The area asymmetry increases dramatically with v for both the enhanced network and active region observations. We explain this result by noting that as the profiles are smeared, an equal amount of each polarity is cancelled, so that the net polarization (the numerator $A_b - A_r$) remains the same (giving the contribution of the line to the broadband polarization in the limit of $v \to \infty$), but the sum of the absolute areas of the Stokes V wings (the denominator $A_b + A_r$) decreases (cf. Fig. 3). The quantity $(A_b - A_r)/(A_b + A_r)$ is therefore bound to increase with increasing spectral smearing.

Indeed the quantity $A_b - A_r$ (what we call the absolute area asymmetry) was found to be constant within our numerical accuracy of a couple of percent, in the range $0 \leq v \leq 150$ mÅ for different solar regions and instrumental profile shapes. We find that the quantity $(A_b - A_r)/S_V$ is practically independent of both resolution and filling factor. S_V has a physical meaning different from $A_b + A_r$, and the insignificant v dependence of $(A_b - A_r)/S_V$ which we find is not simply an artifact, but reflects this difference.

The behaviour of $(a_b - a_r)/(a_b + a_r)$ can be understood in general terms, by considering the following three effects: Firstly, $a_b + a_r$ decreases strongly with v (Fig. 2). This tends to increase the relative amplitude asymmetry. Secondly, the absolute amplitude asymmetry, $a_b - a_r$, decreases initially even more rapidly with v, which is quite contrary to what was observed for the area asymmetry. The main reason for this rapid decrease is that the blue peak, being narrower than the red peak, is more strongly affected by spectral smearing, so that a_b decreases faster than a_r, approaching the latter asymptotically. For large v both peaks are so broad that this effect becomes small, allowing the relative amplitude asymmetry to increase again. Thirdly, due to the overlapping and partial cancellation of the blue and red wings and also due to the general broadening of the Stokes V profile, the blue and red maxima move apart, and no longer necessarily represent the same part of the line.

In contrast to the case of the area asymmetry, the S_V normalised amplitude asymmetry $(a_b - a_r)/S_V$ is not a useful parameter, being strongly resolution dependent. This is because $a_b - a_r$ depends strongly on v while S_V does not.

3.2. *Zero-crossing wavelength*

Figure 4 shows the change in zero-crossing wavelength, $\lambda_V(v) - \lambda_V(0)$, in m s^{-1}, as a function of v. The increase in λ_V is due to the Stokes V asymmetry. Since the blue wing of Stokes V is stronger than its red wing, more of the blue polarity survives spectral smearing and the resulting cancellation of signs, thus pushing the zero-crossing towards the red. Due to the larger asymmetry in our enhanced network Stokes V data, the induced zero-crossing shift is larger for the network than for the strong plage. The effect depends only slightly on the shape of the instrumental profile. This effect may, at least in part, be responsible

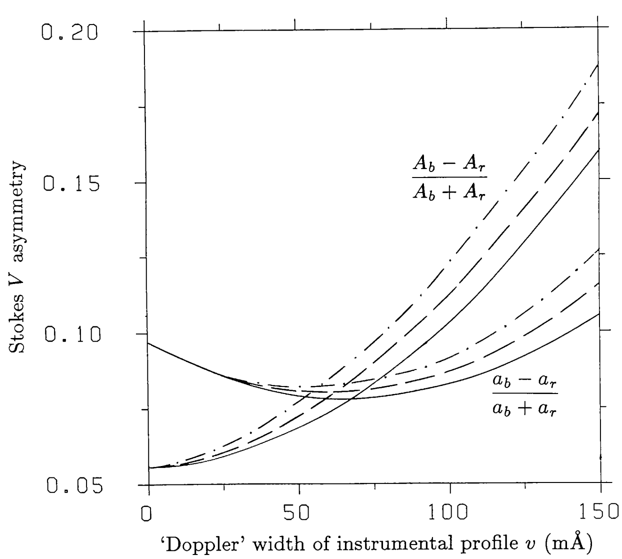

Fig. 3. Relative area asymmetry, $(A_b - A_r)/(A_b + A_r)$, and relative amplitude asymmetry, $(a_b - a_r)/(a_b + a_r)$, of Fe I 5250.2 Å Stokes V vs. v. The three different instrumental profile shapes are represented in the same way as in Fig. 2. The data are from an active region plage

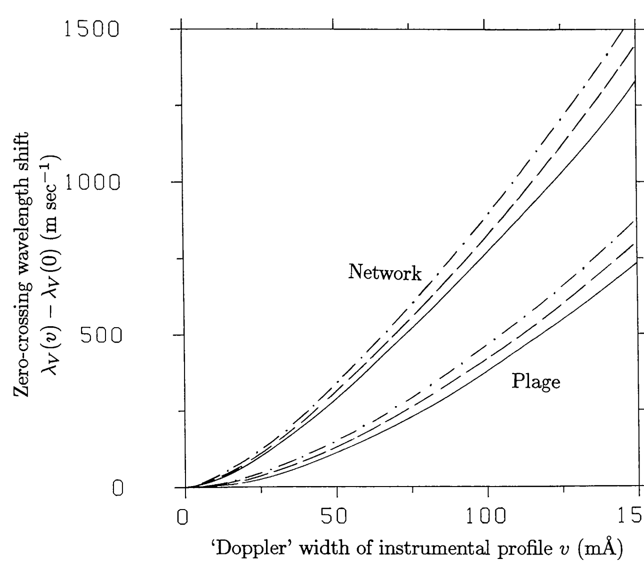

Fig. 4. $\lambda_V(v) - \lambda_V(v = 0)$ in velocity units vs. v. The upper set of curves represents the induced zero-crossing shift for network data smeared with profiles of different shapes (see Fig. 2). The lower set of curves represents plage data

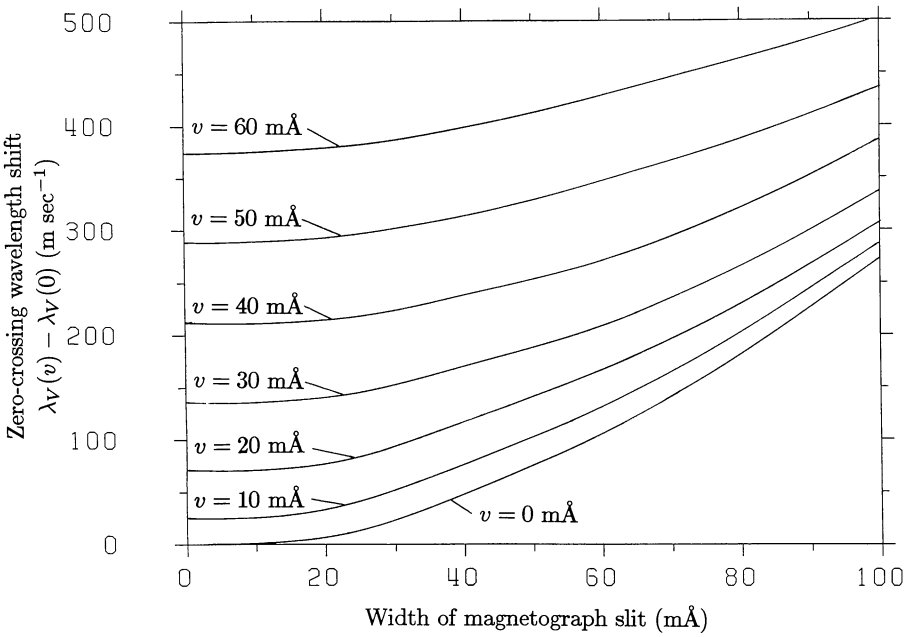

Fig. 5. Zero crossing shift of the Fe I 5250.2 Å line, induced by using the line-centre-magnetogram technique vs. full width of the magnetograph exit slit. From the bottom to the top the curves mark profiles broadened by Gaussian apparatus functions (representing spectrograph entrance slits) with $v = 0$, 10, 20, 30, 40, 50, and 60 mÅ. The diagram represents the enhanced network

for the redshifts seen by Giovanelli and Slaughter (1978), Wiehr (1985a), and Scholier and Wiehr (1985), as was first suggested by Stenflo et al. (1984). We shall discuss this problem in more detail in Sect. 4.

Often the Stokes V redshift is only measured relative to the Stokes I core wavelength, which means that we also have to consider what happens to Stokes I if the spectral resolution is changed. We have therefore convoluted Stokes I with the same instrumental profiles used to smear Stokes V. The I profile is shifted only slightly as a result of spectral smearing, as compared to the shift of Stokes V. The shift increases continuously towards the *blue* for the enhanced network line profile, and reaches a value of approximately $-230\,\mathrm{m\,s^{-1}}$ for $v = 150$ mÅ for a Gaussian apparatus function. It should be compared with the $1330\,\mathrm{m\,s^{-1}}$ by which Stokes V is shifted through the same amount of smearing. For the active region plage, the Stokes I profile first shifts towards the red till it reaches a maximum of about $+60\,\mathrm{m\,s^{-1}}$ at $v = 70$ mÅ, before reversing the trend and shifting towards the blue. It finally reaches a blueshift of approximately $-110\,\mathrm{m\,s^{-1}}$ at $v = 150$ mÅ. This different behaviour of the plage and network wavelengths reflects the difference in the shape of the Stokes I profiles of such regions, as is also reflected in their bisectors (cf. Cavallini et al., 1985).

How strongly does the line-centre-magnetogram technique of Giovanelli and Ramsey (1971) affect the deduced zero-crossing wavelength? The Stokes V zero-crossing wavelength, as determined by this technique, is the wavelength at which the total polarization signal from a single magnetograph slit placed near the centre of the line is zero. Figure 5 shows the zero-crossing wavelength shift in $\mathrm{m\,s^{-1}}$ plotted vs. the width of the magnetograph slit (in mÅ) for data from the enhanced network. The total instrumental profile is in this case composed of a Gaussian (representing the entrance slit and the spectrograph), convoluted with a rectangular profile (exit slit). The lowest curve represents the original FTS data, the other curves are the results for data smeared by Gaussians with $v = 10$, 20, 30, 40, 50, and 60 mÅ, respectively, in the order of increasing redshift (upwards in the figure). The effects of changing the different parameters are clearly visible from the figure, and need not be described further. The results for the active region plage are similar, although the induced shifts are somewhat smaller, due to the smaller asymmetry of the plage Stokes V profile.

4. Application of the results to some observations of Stokes V zero-crossing wavelengths in the literature

Evidence for downflows inside fluxtubes obtained directly from Stokes V has to our knowledge been limited to studies by Giovanelli and Ramsey (1971), Harvey (1977), Giovanelli and Brown (1977), Giovanelli and Slaughter (1978), Wiehr (1985a), and Scholier and Wiehr (1985). However, recent polarimetric data obtained with the Kitt Peak McMath vertical grating-spectrometer as well as with the FTS indicate that no downflows with velocities larger than approximately $250\,\mathrm{m\,s^{-1}}$ are present (Stenflo and Harvey, 1985; Solanki, 1985, 1986). One possible reason for this discrepancy may be the superior spectral resolution of the observations showing no downflows. In the following we shall consider this possibility in somewhat greater detail.

Giovanelli and Ramsey (1971) and Giovanelli and Brown (1977) observed the Ca I 6102.7 Å line with a tunable Fabry-Pérot filter. The width at half maximum of its transmission band is given by Ramsey et al. (1970) as 59 mÅ at 6100 Å. They (Giovanelli and co-workers) measured downflow velocities of around $0.5\,\mathrm{km\,s^{-1}}$ relative to the Stokes I wavelength of the quiet sun. After correcting for the blueshift of Stokes I (Giovanelli and Slaughter, 1978; Dravins et al., 1981) a downflow velocity of approximately 300–$350\,\mathrm{m\,s^{-1}}$ remains.

Since the Ca I 6102.7 Å line is contained in our spectra (in one enhanced network and one plage scan), we could carry out the simulations directly on its profile. A Voigt profile with FWHM $= 60$ mÅ and $a = 0.1$ probably approximates the filter function best, due to its extended wings (Brault, 1982). The zero-crossing shift induced by this profile is $150\,\mathrm{m\,s^{-1}}$. The residual redshift after subtracting this fictitious shift, is still approximately 200 m s^{-1}. This could represent a small downflow, or a small line shift produced by asymmetries in the up and downflow phase of an oscillation (Solanki, 1986), but there are other possible explanations as well. The amount of parasitic light (defined as light which is transmitted outside the 'normal' instrumental profile of the filter) is quite large for the Culgoora filter according to Ramsey et al. (1970). Giovanelli and Brown (1977) also mention that the filter transmission varies with position in the field of view. It is therefore possible that the effective filter function is broader in their actual measurements (which were carried out away from the centre of the field of view). When the filter half width is increased from 60 to 80 mÅ in our simulations, the residual observed shift is reduced to approximately 100 m s^{-1}. Yet another possibility is that the mean asymmetry of the Stokes V profiles in their observed regions is different from the FTS profiles we have used.

Giovanelli and Slaughter (1978) used the Kitt Peak vacuum telescope and magnetograph. The spectral widths of their entrance and exit slits were 47.6 mÅ and 364 mÅ respectively for the IR lines Ca II 8542 Å, Fe I 8688 Å, and C I 9111 Å, and 28 and 215 mÅ respectively for Mg I b_1 5183 Å (Harvey, 1985).

We carried out our simulation of the line-centre magnetogram technique (cf. Sect. 3.2) on the strong Mg I b_1 line directly (it being present in the same FTS scans as Fe I 5250.2 Å), as well as on the Fe I 5250.2 Å line, instead of the weak IR lines measured by Giovanelli and Slaughter, which are not present in our spectra.

The Stokes V profile of the Mg I b_1 line was shifted by less than 100 m s^{-1} towards the red through the instrumental smearing. This is due to the large width and small asymmetry of this line. Since the Fe I 5250 Å line has a much smaller wavelength than the IR lines used by Giovanelli and Slaughter, we assumed that the spectral exit slit width was the same as for the Mg I b_1 line, and not the larger value of the IR lines. Even with the smaller slit widths fictitious redshifts of 900 m s^{-1} and 1400 m s^{-1} were induced for the plage and network profiles, respectively. These values are substantially larger than those observed by Giovanelli and Slaughter (1978), who find the largest downflow for the C I 9111 Å line, with a value of approximately 600–800 m s^{-1}, after correction for Stokes I blueshift. This difference may be due to smaller asymmetries of the line profiles they measure, as compared with the Fe I 5250 Å line. In any case, our simulations easily reproduce the magnitude of the observed zero-crossing shifts.

Wiehr (1985a) has used the Locarno Gregory telescope (Wiehr et al., 1980), with the entrance slit in the form of a circular hole having an angular diameter of 8 arcsec (Wiehr, 1985a). The instrumental profile is found to be a Gaussian with $v = 92$ mÅ (Wiehr, 1985b). From Fig. 4 we see that the redshift induced by such a resolution is 300–350 m s^{-1} for the active region profile of Fe I 5250.2 Å, and 650–700 m s^{-1} for the enhanced network profile. Wiehr observed in isolated Ca II plage elements which correspond more closely to our enhanced network elements than to a strong active region plage. We can check this by comparing the Stokes V asymmetry of Wiehr's line profiles with ours, since the asymmetry is the primary cause of the induced redshift. We find that the average amplitude asymmetry of Wiehr's observations is $\langle a_b/a_r \rangle = 1.69$. If corrected for spectral degradation this gives $\langle a_b/a_r \rangle (v = 0) = 1.86$, which is closer to the asymmetry of our network observations than to our plage observations. If we also take into account the fact that the wavelength of the Stokes I profile with which Wiehr compares the Stokes V wavelength is blueshifted by 150–350 m s^{-1} (Dravins et al., 1981), the total fictitious redshift becomes of the order of 800–1000 m s^{-1}, which compares very well with the 900 m s^{-1} average redshift he measures.

5. Summary and conclusions

We have attempted to catalogue some of the effects of low spectral resolution on the Stokes V profile. The variation of the amplitude, area, asymmetry, and zero-crossing wavelength of the Fe I 5250.2 Å line with the width of the instrumental profile has been studied. As one application of these results we have given strong quantitative evidence that the sometimes large observed redshifts of Stokes V are induced by the interplay between Stokes V asymmetry and low spectral resolution. Thus the observations of Giovanelli and co-workers (1971, 1977, 1978) and of Wiehr (1985a) have been discussed in some detail. The approximate magnitude of the effect observed by them can be reproduced in each case by our simulations.

Regarding one of the remaining observations of downflow in Stokes V (Harvey, 1977), we have been informed by Harvey (1985) that subsequent measurements of the same line with the same instrumental setup failed to reproduce the earlier results. It would therefore be highly desirable to carry out further observations in the infrared region around 16000 Å to clarify this point. In the other undiscussed observation, Scholier and Wiehr (1985) find a redshift of Stokes V relative to Stokes I in three magnetic regions and a blueshift in only one region (region D in their Fig. 8). However, as Wiehr (1985b) informs us, analysis of a number of further regions yielded both blue- and redshifts. Thus the average shift of all the regions should not differ strongly from zero. We therefore conclude that the observations in the literature are all compatible with a *mean* downflow velocity of less than 250 m s^{-1} throughout the photospheric layers of fluxtubes, as suggested by the analyses of Stenflo and Harvey (1985) and Solanki (1985, 1986). The absence of downflows in fluxtubes is also supported by the results of centre-to-limb variation studies of the Stokes V zero-crossing wavelength carried out by Stenflo et al. (1986).

Acknowledgements. We are greatly indebted to M.C.E. Huber for many clarifications, to J.W. Harvey for providing us with data on the Kitt Peak vacuum telescope and for fruitful discussions, and to H. Wöhl, W. Mattig, and E.H. Schröter for helpful comments. It is also a pleasure to thank E. Wiehr for providing valuable information on his observations, and for a critical reading of the manuscript. The work of one of us (SKS) was supported by grants No. 2.814-0.83 and 2.666-0.85 from the Swiss National Science Foundation.

References

Allen, C.W.: 1973, *Astrophysical Quantities*, Athlone Press, London, pp 86–89

Brault, J.W.: 1982, *Phil. Trans. Roy. Soc. London A* **307**, 503

Cavallini, F., Ceppatelli, G., Righini, A.: 1985 *Astron. Astrophys.* **143**, 116

Dravins, D., Lindegren, L., Nordlund, Å.: 1981, *Astron. Astrophys.* **96**, 345

Giovanelli, R.G., Ramsey, J.V.: 1971, in R. Howard (ed.) *Solar Magnetic Fields*, *IAU Symp.* **43**, 293

Giovanelli, R.G., Brown, N.: 1977, *Solar Phys.* **52**, 27

Giovanelli, R.G., Slaughter, C.: 1978, *Solar Phys.* **57**, 255

Harvey, J.W.: 1977, in *Highlights of Astronomy*, E.A. Müller (Ed.), Vol. 4, Part **II**, 223

Harvey, J.W.: 1985, private communication

Mihalas, D.: 1978, *Stellar Atmospheres*, Freeman and Company, San Francisco, pp 279–281

Ramsey, J.V., Kobler, H., Mugridge, E.G.V.: *Solar Phys.* **12**, 492

Scholier, W., Wiehr, E.: 1985, *Solar Phys.* **99**, 349

Solanki, S.K.: 1985, in H.U. Schmidt (Ed.), *Theoretical Problems in High Resolution Solar Physics*, MPA, Munich, 172

Solanki, S.K.: 1986, *Astron. Astrophys.* (in press)

Solanki, S.K., Stenflo, J.O.: 1984, *Astron. Astrophys.* **140**, 185

Solanki, S.K., Stenflo, J.O.: 1985, *Astron. Astrophys.* **148**, 123

Stenflo, J.O., Harvey, J.W.: 1985, *Solar Phys.* **95**, 99

Stenflo, J.O., Harvey, J.W., Brault, J.W., Solanki, S.K.: 1984, *Astron. Astrophys.* **131**, 333

Stenflo, J.O., Solanki, S.K., Harvey, J.W.: 1986, *Astron Astrophys.* (in press)

Unsöld, A.: 1955 *Physik der Sternatmosphären*, Springer Verlag, Berlin

von Alvensleben, A.: 1957, *Z. Astrophys.* **43**, 63

Wiehr, E.: 1985a, *Astron. Astrophys.* **149**, 217

Wiehr, E.: 1985b, private communication

Wiehr, E., Wittmann, A., Wöhl, H.: 1980, *Solar Phys.* **68**, 207